Sparse Unmixing With Dictionary Pruning for Hyperspectral Change Detection

Alp Ertürk, *Member, IEEE*, Marian-Daniel Iordache, and Antonio Plaza, *Fellow, IEEE*

***Abstract*—The localization of changes that occur between the images in a multitemporal series is crucial for many applications, ranging from environmental monitoring to military surveillance. In contrast to traditional change detection methods, unmixing-based change detection has been shown to have the important added benefit of providing subpixel-level information on the nature of the changes, instead of only providing the location of the changes. Recently, sparse unmixing has also been introduced to hyperspectral change detection, resulting in a method that circumvents the drawbacks of regular spectral unmixing approaches. Sparse unmixing-based change detection reveals the changes that occur in a multitemporal series, at subpixel level, and in terms of the library spectra and their sparse abundances, and provides enhanced change detection performance, especially when subpixel-level changes have occurred. However, sparse unmixing is generally an ill-conditioned and time-consuming process, especially as the size of the utilized spectral library increases. In this paper, dictionary pruning is exploited for the first time for hyperspectral change detection using sparse unmixing, in order to alleviate the ill-conditioning of the problem and achieve decreased computation times and enhanced change detection performance. Experimental results on both realistic synthetic and real datasets are used to validate the proposed approach.**

***Index Terms*—Change detection, dictionary pruning, hyperspectral imaging, multitemporal, sparse unmixing.**

I. Introduction

HYPERSPECTRAL change detection is defined as the process of detecting the changes that occur in a multitemporal hyperspectral image series acquired from the same scene at different times. These changes can occur due to the passage of time, as a result of seasonal/diurnal variation, or may result from a significant event such a natural disaster [1]. Change detection for hyperspectral images is crucial for many application fields such as urban planning, environmental monitoring, precision agriculture, or defense.

There are a large number of existing change detection methods for multitemporal multispectral or hyperspectral imagery. Chronochrome (CC) [2] and covariance equalization (CE) [3], which are, respectively, a linear predictor to calculate the linear transformation matrix between the two images using second-order statistics, and a similar method based on whitening, which does not utilize cross-covariance matrix in order to reduce sensitivity to misregistration, can still be considered the benchmark change detection methods. Hyperbolic anomaly change detector (HACD) [4] is a method that combines these linear predictors in a general framework, and aims to detect anomalous changes. Other change detection methods include subspace-based change detection [5], which computes and uses the background subspace in one image to detect the changes in another image, and multivariate alteration detection (MAD) [6] and iteratively reweighted MAD [7], which aim to detect the changes using the canonical variates.

While there are a large number of change detection methods in the literature, most (if not all) such methods operate on a pixel-level basis, and require modifications to be able to provide subpixel-level change detection outputs. In addition, none of those methods provide the information about the actual nature of the change. In light of these points, unmixing-based change detection comes to forefront.

Unmixing is the process of decomposing each pixel of a hyperspectral image into a set of fractional abundances of endmember signatures [8]. A thorough review of the different approaches and methods for unmixing can be found in [9]. A recent addition, unmixing-based change detection provides subpixel-level change detection outputs and had the added benefit of providing easy to interpret information on the nature of the changes that have occurred. This information on the "nature" can be in terms of a sudden increase in the abundance of an endmember, such as water, for natural disasters, change in the type of cultivated crop or a change in the stress levels for crops in a farmland, new anomalous endmembers in the scene for target detection, and so on. A general framework for change detection by spectral unmixing has been proposed in [10], whereas a case study on subpixel-level change detection by unmixing is presented in [11], and land-cover mapping by unmixing is discussed in [12]. In a recent paper, unmixing-based change detection, and the benefits it provides have been examined and presented in detail [13]. Similar benefits have been highlighted in a very recent paper, which proposes multitemporal unmixing with a patch scheme for change detection [14]. These techniques all rely on a traditional (unsupervised) spectral unmixing approach based on dimensionality reduction followed by image-based endmember extraction. In another recent paper, sparse unmixing has been utilized for the first time in unmixing-based change detection for multitemporal hyperspectral

Manuscript received December 23, 2015; revised May 16, 2016 and August 17, 2016; accepted September 1, 2016. Date of publication October 4, 2016; date of current version December 22, 2016. *(Corresponding author: Alp Ertürk.)*

A. Ertürk is with Kocaeli University Laboratory of Image and Signal Processing, Kocaeli University, Kocaeli 41380, Turkey (e-mail: alp.erturk@kocaeli.edu.tr).

M.-D. Iordache is with the Flemish Institute for Technological Research (VITO), Center for Remote Sensing and Earth Observation Processes (TAP), Mol 2400, Belgium (e-mail: marian-daniel.iordache@vito.be).

A. Plaza is with the Hyperspectral Computing Laboratory, Department of Technology of Computers and Communications, University of Extremadura, Cáceres E-10003, Spain (e-mail: aplaza@unex.es).

Color versions of one or more of the figures in this paper are available online at http://ieeexplore.ieee.org.

Digital Object Identifier 10.1109/JSTARS.2016.2606514

images [15]. In this case, the unmixing approach is driven by the use of a spectral library that is assumed to contain ideal endmembers. This introduces a fundamental difference with the change detection techniques based on traditional spectral unmixing, in which the endmembers (and their number) need to be estimated in advance, while in sparse unmixing the endmembers are assumed to be available in the library, which is exploited in semisupervised fashion to perform the unmixing of the scene.

In fact, sparse unmixing aims to detect an optimal subset of signatures from a potentially large spectral library to accurately and efficiently model the hyperspectral data at hand [16], [17]. A sparsity-inducing regularizer function is most commonly used to keep the number of selected signatures as small as possible. Sparse unmixing has gained much attention in recent years with the increase in the availability and scope of spectral libraries. Sparse unmixing via variable splitting augmented Lagrangian (SUnSAL) [18] is still considered the benchmark sparse unmixing method. However, sparse unmixing methods that also utilize spatial information have recently started to become more prominent. Among such methods, sparse unmixing via variable splitting augmented Lagrangian and total variation (SUnSAL-TV) [19], which includes spatial information by means of a TV regularizer [20], and nonlocal sparse unmixing [21], which uses spatial information to derive possible predictions in the abundance maps, can be counted.

Sparse unmixing-based change detection using spectral libraries, introduced in [15], provides subpixel-level change detection, and information on the nature of the changes between the temporal datasets in terms of endmembers and abundances. The approach also provides increased change detection performance with respect to conventional change detection methods, especially when there are subpixel-level variations [15].

While sparse unmixing has many advantages, it is also an ill-conditioned and time-consuming problem due to the large sizes and high coherences, i.e., high similarities between the contained signatures, of the spectral libraries. To address this shortcoming, in a recent paper, the fact that hyperspectral images can be represented in a lower dimensional subspace with small information loss has been utilized to detect a subset of the spectral library to be used in sparse unmixing [22]. Using this subset of the spectral library with sparse unmixing for the data has been shown to improve the conditioning of the process, and decrease the high similarity of the signatures in the spectral library, therefore decreasing computation times while also enhancing performances [22].

This paper introduces dictionary pruning for sparse unmixing-based change detection in hyperspectral images. The proposed approach alleviates the ill-conditioning of the unmixing process, and achieves reduced computation time and enhanced change detection performance.

The remainder of this paper is organized as follows. The proposed methodology is presented in Section II. Experimental results for synthetic and real datasets are provided in Section III and Section IV, respectively. Section V concludes the paper with hints at plausible future studies.

II. Methodology

In this paper, sparse unmixing with dictionary pruning is proposed for change detection in multitemporal hyperspectral images. The proposed method can be used with any spectral library. However, the spectral signatures in the spectral library need to be matched to the data in terms of characteristics. For this reason, in this paper, two preprocessing steps are applied to spectral libraries before dictionary pruning. First, the number of spectral bands of the signatures in the library is reduced to match the number of bands of the hyperspectral datasets, as generally the number of bands for the library signatures is significantly higher than those of hyperspectral datasets. This reduction is done by a nearest neighbor approach in the spectral axis, such that for each signature in the library, the spectral bands with the wavelengths that most closely match the wavelengths of the spectral bands of the data are selected, and the rest of the bands are eliminated. As this step may cause discontinuities in the resulting signatures, the second preprocessing step is used, in which a simple Gaussian filter is used to smooth out the resulting spectral signatures.

After these preprocessing steps have been conducted, dictionary pruning is applied to the spectral library with the signatures that match the data characteristics. This dictionary pruning process is mostly similar to the process proposed in [22], and is repeated here for completeness. Dictionary pruning process is as follows.

1) The subspace dimensionality of the data is estimated using the hyperspectral subspace identification by minimum error (HySime) [23]. In this paper, the dimensionality is estimated from the whole multitemporal hyperspectral datasets acquired from a scene, in conjunction, instead of from each temporal dataset separately, as the dictionary will be pruned once for all the temporal datasets. For this purpose, temporal hyperspectral images are spatially merged into a single data stack.
2) The spectral signatures of the library are orthogonally projected onto the eigenvectors of the subspace detected in the first step.
3) Projection error is computed for each library signature based on normalized Euclidian distance.
4) A subset of the spectral library is retained based on projection error. In this paper, a fixed threshold as in [17] is not used for this purpose, due to the variability of the errors. Instead, a percentage of the library is retained, starting from the signature with the lowest projection error. This percentage has been fixed to 25% throughout this paper, for simplicity.

After the dictionary pruning process is completed, sparse unmixing with the pruned spectral library is applied to the multitemporal hyperspectral data stack. This ensures that the sparse solutions do not vary greatly for the temporal datasets. In this paper, SUnSAL-TV is selected as the sparse unmixing method, as it integrates spatial processing into the unmixing progress, and hence provides increased performance with respect to more regular sparse unmixing approaches. SUnSAL-TV solves the following optimization problem under the linear mixture model

assumption:

$$\min_{\boldsymbol{X}} \frac{1}{2} \|\boldsymbol{A}X - \boldsymbol{Y}\|_F^2 + \lambda \|\boldsymbol{X}\|_{1,1} + \lambda_{\mathrm{TV}} \mathrm{TV}(\boldsymbol{X}) \quad (1)$$

$$\text{subject to } \boldsymbol{X} \geq 0$$

$$\mathrm{TV}(\boldsymbol{X}) \equiv \sum_{\{i,j\} \in \varepsilon} \|\boldsymbol{X}_i - \boldsymbol{X}_j\|_1 \quad (2)$$

where ε denotes the set of neighbors, $\mathbf{A}$ denotes the spectral library, $\mathbf{Y}$ is the observed data, and $\boldsymbol{X}$ is the abundance matrix, such that the abundance vector of pixel i is $\boldsymbol{X}_i$. The first term in (1) aims to keep the reconstruction error low, the second term aims to keep the abundance matrix sparse, while the third term promotes smooth transitions in the abundances for neighboring pixels. In this paper, the maximum number of iterations for SUnSAL-TV was fixed to 200 in each test, for simplicity. Note that it is possible to achieve better performances by increasing the number of iterations, at the cost of computation time.

The sparse abundance matrix outputs of SUnSAL-TV are then assigned into the corresponding temporal datasets. After this step, changes between the temporal datasets are revealed through the differences in their respective abundance maps for each library spectral signature that exists in the sparse solution for the multitemporal dataset. The variation for a material can be obtained by a simple difference operation on the abundance maps obtained for each temporal dataset for that material's library signature. An overall change map is constructed by simple summation of each abundance variation map.

The proposed methodology can be used with any spectral library. However, as expected, the performance would be better with a spectral library that closely relates to the multitemporal dataset (and the sensor used to acquire the data) with respect to a spectral library that does not have much in common with the data at hand. In addition, while the approach could be used for raw data, atmospherically corrected data are more relatable to the library spectra collected in the laboratory environment, and therefore better performances would be obtained for atmospherically corrected data, as in this paper.

III. Experimental Results on Synthetic Data

A. Synthetic Dataset 1

A synthetic multitemporal hyperspectral dataset is simulated from the AVIRIS Salinas dataset to be used in the experimental results. Salinas is originally sized 512 × 217 pixels, with 224 spectral bands. Its spatial resolution is 3.7 m. The original dataset and ground-truth information are available online in [24].

In this paper, a subset of the Salinas image is selected as the first temporal hyperspectral dataset. The selected area is 217 × 217 pixels. Water absorption bands have been eliminated, resulting in 204 spectral bands. The second temporal dataset is simulated from the first dataset by modifying some pixels of the data. The modified pixels are in the "grapes_untrained" class, and the modification is done by changing each pixel in the "grapes_untrained" labeled regions to a randomly selected pixel from the "vineyard_untrained" labeled section. RGB images of the resulting temporal datasets are presented and the modified locations are indicated in Figs. 1 and 2.

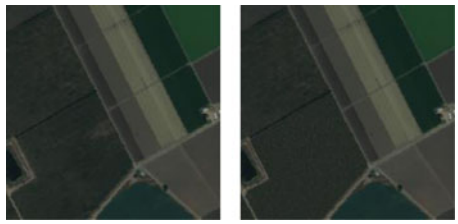

Fig. 1. RGB images for the multitemporal Salinas dataset.

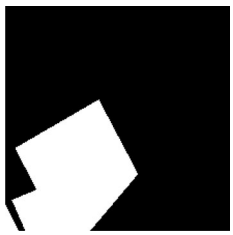

Fig. 2. Change ground truth for the multitemporal Salinas dataset.

For the evaluation of sparse unmixing-based approaches, a spectral library is constructed from the vegetation and man-made signatures of the U.S. Geological Survey (USGS) spectral library, for a total library size of 310. λ and λ_{TV} regularization parameters of SUnSAL-TV have been set as 0.001 and 0.1, after a crude empirical analysis.

In this case study, the changes between the temporal datasets are purely at pixel level with no subpixel-level variation involved. Hence, it should be expected that the traditional methods will also perform well in terms of overall change detection performance. However, the conducted change is quite challenging, as the exchanged pixels are from very similar classes, both in terms of RGB values, and spectrally. In addition, before processing for change detection, additive Gaussian white noise is added to each temporal dataset in 30 dB SNR to make the problem more challenging.

Sparse unmixing-based approaches are compared with traditional change detection methods of change vector analysis (CVA), spectral angular distance (SAD), CC, CE, and HACD.

Fig. 3 gives a comparison between the final change maps obtained by each method. Note that the change maps for the sparse unmixing-based approaches are obtained by the summation of abundance change map obtained for each library spectra. ROC curves based on the ground-truth change map are provided in Fig. 4.

It can be observed from the ROC curves that among the traditional methods, HACD performs the best overall. However, the highest performances are achieved with sparse unmixing-based change detection approaches. It can also be observed that the proposed approach involving dictionary pruning enhances change detection performance by improving the conditioning of the problem. This can also be observed from the higher area under curve (AUC) values that the proposed methodology provides, which are derived from the ROC curves and are presented

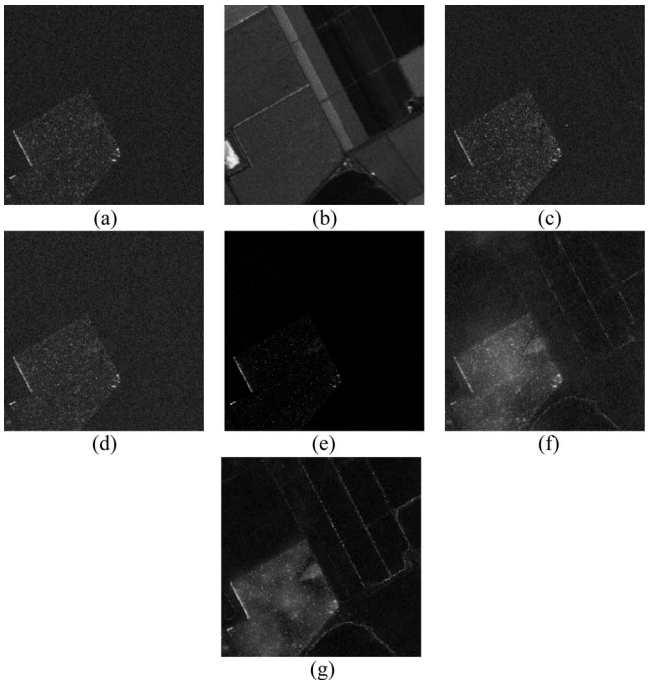

Fig. 3. Final change maps for Salinas by (a) CVA, (b) SAD, (c) CC, (d) CE, (e) HACD, (f) sparse unmixing, and (g) proposed.

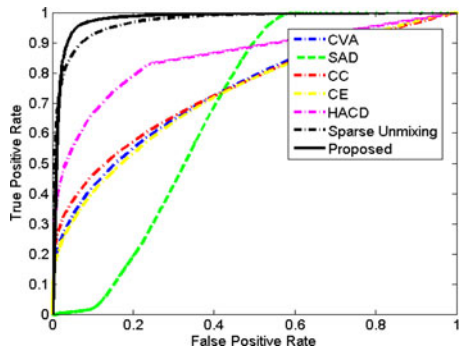

Fig. 4. ROC curves for the Salinas.

TABLE I
AUC VALUES AND RUNTIMES FOR SALINAS

Method	AUC values	Runtime (s)
CVA	0.7406	1.6
SAD	0.6743	2.2
CC	0.7466	0.3
CE	0.7323	0.3
HACD	0.8546	1.7
Sparse unmixing	0.9723	2120
Proposed	**0.9800**	560

in Table I. Also provided in Table I are the runtimes of each method, evaluated on MATLAB platform on a computer with 16 GB RAM and i7-4700 HQ with dual 2.4 GHz processors. The proposed method with the dictionary pruning step significantly reduces the computation times for change detection by sparse unmixing. Note that the dictionary pruning step itself constitutes less than 1% of the proposed method's computation time, in this and all the following cases.

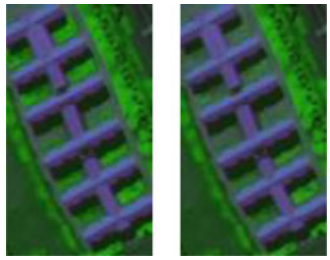

Fig. 5. False color images for the multitemporal Pavia dataset.

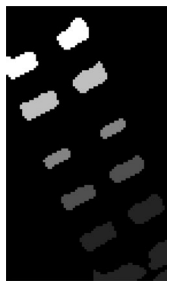

Fig. 6. Change ground truth for the multitemporal Pavia dataset.

B. Synthetic Dataset 2

The second synthetic multitemporal hyperspectral dataset is simulated from the ROSIS Pavia University dataset. Pavia University is originally sized 120 × 70 pixels, with 103 spectral bands. Its spatial resolution is 1.3 m, whereas the spectral resolution is 4 nm.

In this paper, the area in the Pavia University image that contains the metal building is selected as the first temporal hyperspectral dataset. Then, the vegetation regions located between the parts of the building are modified to dirt regions such as those located around the building, in order to obtain the second temporal dataset. This modification process is done in subpixel level and gradually such that, diagonally, the upper left parts of the image are modified more significantly, whereas the lower right parts are modified less significantly. Hence, the variations between the temporal datasets are at varying subpixel levels. False color images of the resulting temporal datasets are provided in Fig. 5, and the modified locations with indication on their modification strength are visualized in Fig. 6. Additive Gaussian white noise is added to each temporal dataset in 30 dB SNR again, before processing to make the problem more realistic.

The spectral library for the sparse unmixing-based approaches is constructed from the USGS spectral library, with vegetation and man-made signatures, for a total spectra size of 310. λ and λ_{TV} regularization parameters of SUnSAL-TV have been set as 0.001 and 0.01, after a crude empirical analysis. Note that the λ_{TV} parameter is smaller in this test case with respect to the previous case, as the spatial smoothness is less pronounced in this image, with respect to the previous Salinas dataset.

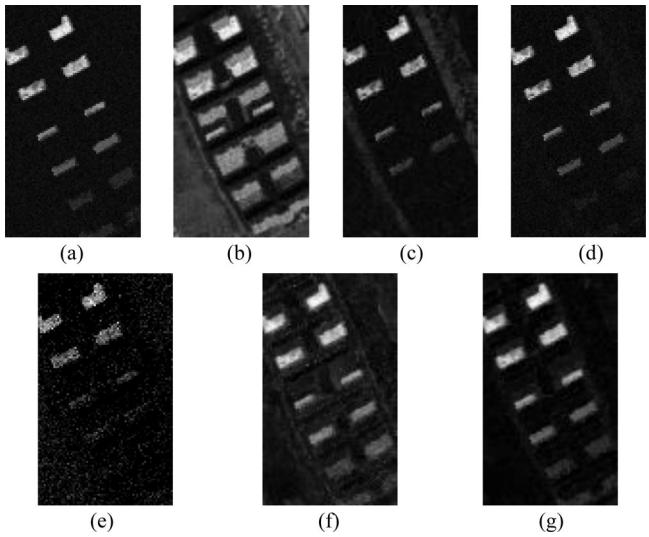

Fig. 7. Final change maps for the Pavia dataset by (a) CVA (b) SAD, (c) CC, (d) CE, (e) HACD, (f) sparse unmixing, and (g) proposed.

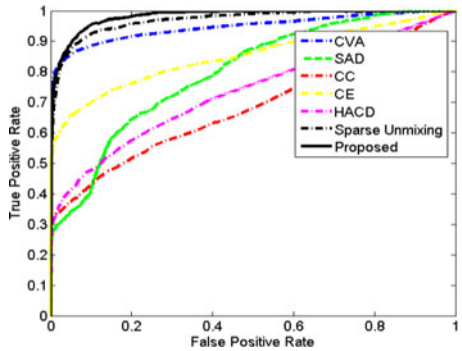

Fig. 8. ROC curves for the Pavia dataset.

TABLE II
AUC VALUES AND RUNTIMES FOR PAVIA

Method	AUC values	Runtime (s)
CVA	0.9485	0.27
SAD	0.7986	0.35
CC	0.6875	<0.1
CE	0.8522	<0.1
HACD	0.7360	0.19
Sparse unmixing	0.9709	390
Proposed	**0.9832**	100

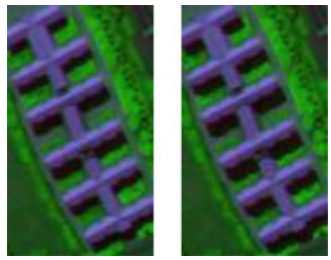

Fig. 9. False color images for the Pavia-Shadow dataset.

Fig. 10. Change ground truth for the Pavia-Shadow dataset.

The final change maps are presented in Fig. 7, and the ROC curves based on the ground-truth change map are provided in Fig. 8. It can be observed that the simple CVA method provides good performance for this case as the variation between the temporal dataset is easy to observe in terms of color or brightness. The other traditional methods have performed considerably worse, as can be seen from Fig. 8, especially as the subpixel variation becomes less pronounced, as can be observed from Fig. 7. The highest performances are achieved with change detection by sparse unmixing approaches, especially with the method including dictionary pruning, which enhances the performance by reducing the dictionary size and improving the conditioning of the problem. This can also be observed from the AUC values derived from these ROC curves that are presented in Table II, along with the runtimes. The proposed method with the dictionary pruning step once again significantly reduces the computation times with respect to change detection by sparse unmixing, in addition to enhancing the performance.

C. Synthetic Dataset 3

The third synthetic multitemporal hyperspectral dataset is also simulated from the ROSIS Pavia University dataset. The same region of the image is used as the previous experimental study, but this is a special case study, in that the change in the scene is caused by the variation of shadow lengths. This case study is aimed to show how each methods copes with shadow variations. Note that the conducted changes are pixel level, so traditional methods are expected to work as well as any unmixing approach. False color images of the temporal datasets are provided in Fig. 9, and the modified locations, i.e., the ground-truth change map, are visualized in Fig. 10. Additive Gaussian white noise is added to each temporal dataset in 30 dB SNR before processing to make the problem more realistic.

The spectral library for the sparse unmixing-based approaches is constructed from the USGS spectral library, with vegetation and man-made signatures, for a total spectra size of 310. λ and λ_{TV} regularization parameters of SUnSAL-TV have been set as 0.001 and 0.01.

The final change maps are presented in Fig. 11, and the ROC curves based on the ground-truth change map are provided in Fig. 12. AUC values are derived from these ROC curves that are presented in Table III, along with the runtimes. As the variation between the temporal datasets is pixel-level shadow effect, CVA performs admirably well, along with the traditional

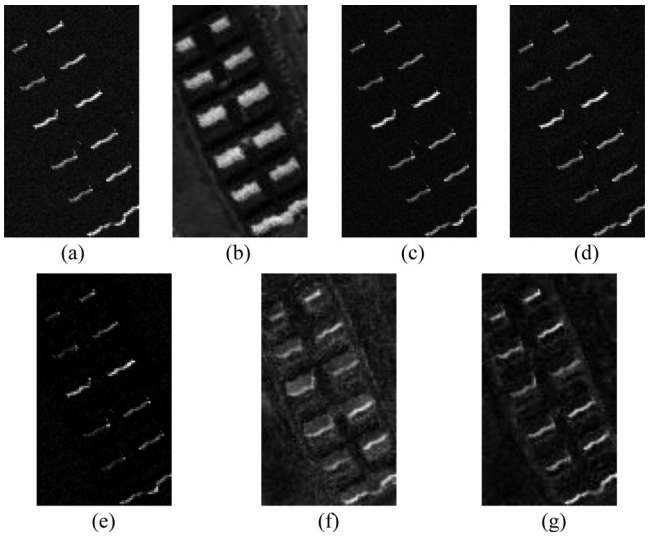

Fig. 11. Final change maps for the Pavia-Shadow dataset by (a) CVA (b) SAD, (c) CC, (d) CE, (e) HACD, (f) sparse unmixing, and (g) proposed.

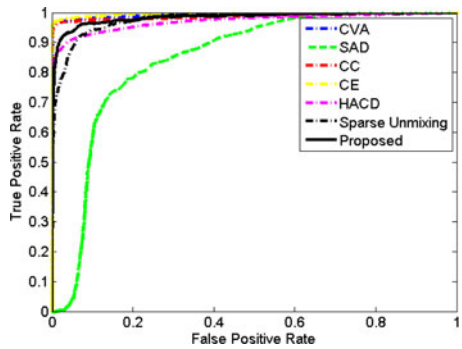

Fig. 12. ROC curves for the Pavia-Shadow dataset.

TABLE III
AUC VALUES FOR AND RUNTIMES FOR PAVIA-SHADOW

Method	AUC values	Runtime (s)
CVA	0.9931	0.26
SAD	0.8450	0.34
CC	0.9886	<0.1
CE	**0.9960**	<0.1
HACD	0.9718	0.19
Sparse unmixing	0.9778	335
Proposed	0.9843	86

methods of CC and CE. Sparse unmixing-based approaches have performed slightly worse in this case, as the spectral library does not include a signature specifically for shadow, as to be expected. Nevertheless, it can be observed that the proposed approach enhances the performance of sparse unmixing-based change detection. The proposed method also significantly reduces the computation times with respect to change detection by sparse unmixing.

It should be noted that, in some cases, the detection of shadow variations is not desired. If the utilized spectral libraries could contain a spectral signature for shadows, then the shadow changes would ideally be obtained specifically due to an abundance variation of this signature, which in turn could be eliminated. However, the spectral signature of areas with shadow depends on what causes the shadow and on what the shadow falls. As such, a specific library spectrum for shadow cannot be obtained. Instead, to prevent the detection of shadow variations in the multitemporal data as changes, a shadow detection [25], [26] or deshadowing [27], [28] algorithm can be used prior to the proposed methodology to mask out the shadow areas.

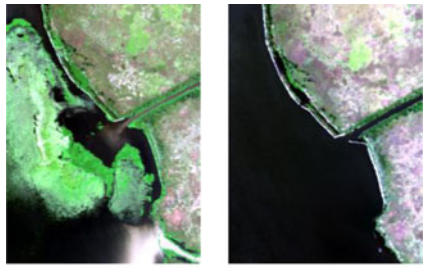

Fig. 13. RGB images for New Orleans dataset: (a) 2010 and (b) 2011.

IV. EXPERIMENTAL RESULTS ON REAL DATA

A. Real Dataset 1

Two hyperspectral datasets that are available in the online AVIRIS database have been utilized for the first experimental study on real data. The respective datasets are acquired in September 2010 and October 2011 from New Orleans, USA. RGB images of the temporal datasets are provided in Fig. 13. Twenty noisy bands have been eliminated before processing.

Using the vegetation and volatiles signatures from the USGS spectral library, a spectral library of 224 spectra has been constructed for the sparse unmixing-based approaches. λ and λ_{TV} regularization parameters of SUnSAL-TV have been set as 0.001 and 0.01, after a crude empirical analysis.

The change maps obtained by CVA, SAD, CC, CE, HACD, sparse unmixing and sparse unmixing with dictionary pruning are provided in Fig. 14.

A ground-truth change map has been prepared for this multitemporal dataset, based on difference operators on false color space, thresholding, and binary morphology. It should be noted that the authors do not claim that the presented ground-truth map is perfect or 100% correct. However, this ground-truth map enables a quantitative assessment of the performances for the respective methods. The ground-truth map, and the ROC curves obtained based on this map are provided in Fig. 15.

For this dataset, CVA, SAD, CE, and the sparse unmixing-based approaches provide relatively similar results, as the change in the scene is relatively easy to detect. Whereas SAD provides slightly better performance overall, the proposed approach enhances the performance of sparse unmixing-based change detection by the added dictionary pruning step, while also reducing average computation time from 5550 to 1660 s, of which the dictionary pruning step itself takes around 9 s.

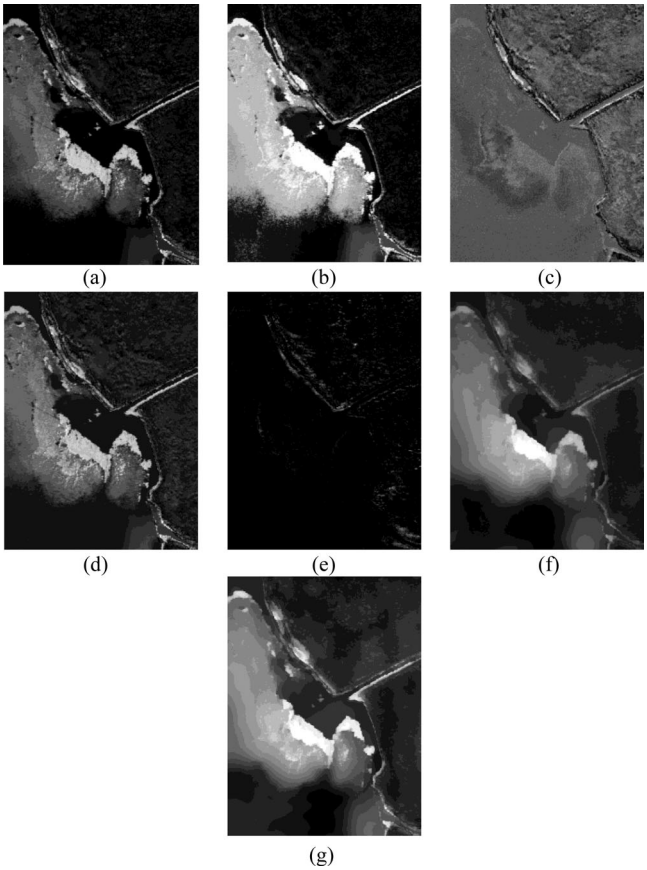

Fig. 14. Final change maps for the New Orleans dataset by (a) CVA (b) SAD, (c) CC, (d) CE, (e) HACD, (f) sparse unmixing, and (g) proposed.

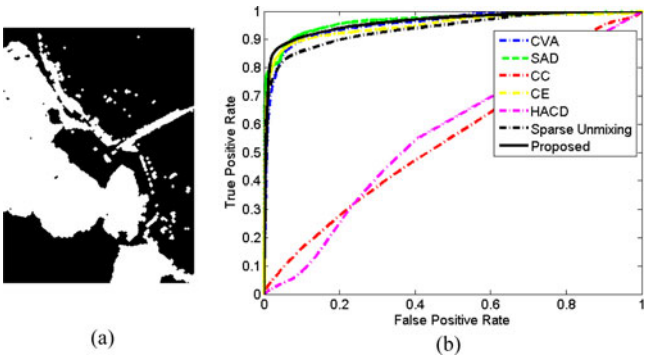

Fig. 15. Quantitative performance assessment for New Orleans dataset: (a) ground-truth map and (b) ROC curves.

B. Real Dataset 2

APEX data acquired over Kalmthout, Belgium, are utilized for the second real data experimental study. A forest fire that has occurred in 23/05/2011 in Kalmthout is the primary interest in this case study. Two different hyperspectral datasets acquired in consecutive flights in June 2010 are spatially mosaicked to construct the first temporal dataset. The second temporal dataset is acquired in June 2011, in a single flight. This variation in flight lines is a direct result of the aforementioned fire, in that the data acquisition flight lines have been

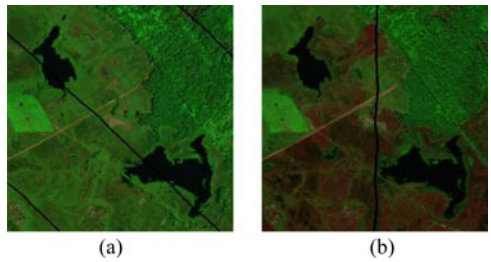

Fig. 16. False color images for Kalmthout dataset: (a) 2010 and (b) 2011.

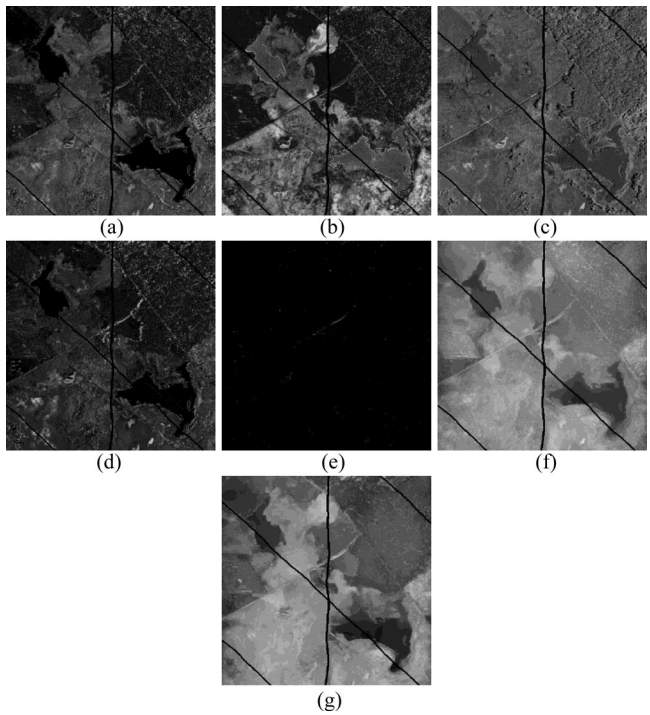

Fig. 17. Final change maps for the Kalmthout dataset by (a) CVA (b) SAD, (c) CC, (d) CE, (e) HACD, (f) sparse unmixing, and (g) proposed.

modified after the fire date to contain the area of interest in a single flight line. The temporal datasets have been cut to 400×400 pixels sizes for computational concerns. Both temporal datasets originally have 295 spectral bands, but the bands with very low SNR are eliminated in this paper, resulting in 245 spectral bands. False color images of the temporal datasets are provided in Fig. 16.

λ and λ_{TV} regularization parameters of SUnSAL-TV have been set as 0.001 and 0.1. A spectral library is constructed from the vegetation and volatiles signatures of the USGS spectral library for a total number of 224 spectra. It should be once again stressed that a dedicated spectral library with more relatable signatures would result in a more enhanced and more informational result with the sparse unmixing-based change detection approaches.

The final change maps obtained by CVA, SAD, CC, CE, HACD, sparse unmixing, and the proposed method are presented in Fig. 17. Note that the interferers resulting from the flight lines were removed from each change map by a simple postprocessing step.

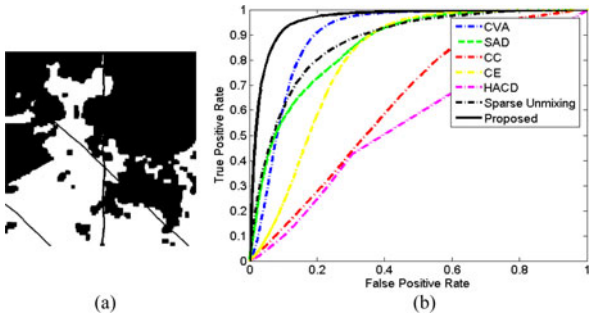

Fig. 18. Quantitative performance assessment for Kalmthout dataset: (a) ground-truth map and (b) ROC curves.

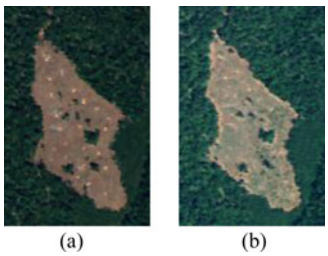

Fig. 19. False color images for Blodgett dataset: (a) 2007 and (b) 2013.

A ground-truth map has been prepared for the multitemporal dataset, based on difference operators on false color space, thresholding, and binary morphology. Whereas it should be noted that this ground-truth map is in no way canon or perfect, it nevertheless enables a quantitative assessment of the performances for the methods utilized in this paper. A minor point of note is that as the ground-truth map is prepared based on intensity differences in the color spaces, it may be acting in favor of CVA.

The ground-truth map for the datasets and the ROC curves computed based on this ground-truth map are provided in Fig. 18. It can be observed that the proposed approach significantly enhances the change detection performance with respect to change detection by sparse unmixing, and provides the best performance overall.

The second benefit of the proposed approach is the reduced computation time with respect to sparse unmixing-based change detection. For this case, the computation times have been reduced on from 7690 to 2270 s. The dictionary pruning step itself costs 16 s on average.

C. Real Dataset 3

Two hyperspectral datasets that are available in the online AVIRIS database have been utilized for the third experimental study on real data. The respective datasets are acquired in 2007 and 2013 from the Blodgett region, Oregon, USA. The temporal datasets have been reduced to 180 $\times$ 120 pixels for computational concerns. RGB images of the temporal datasets are provided in Fig. 19.

Several green areas from the 2007 data are not present anymore in the 2013 data, most probably due to (natural or man-made) removal of trees. However, vegetation appears in other

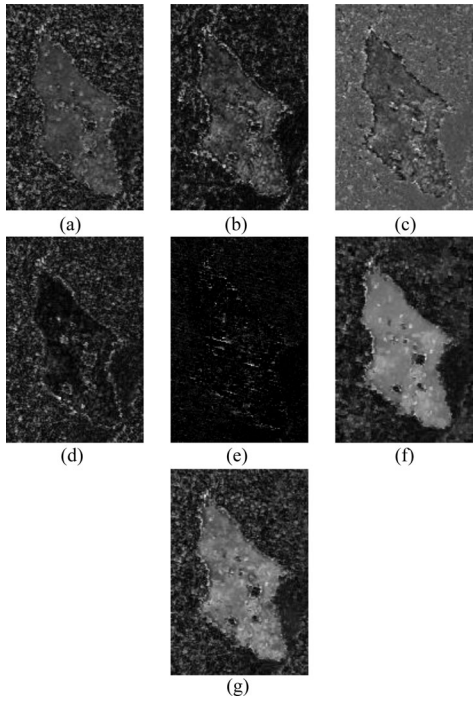

Fig. 20. Final change maps for the Blodgett dataset by (a) CVA (b) SAD, (c) CC, (d) CE, (e) HACD, (f) sparse unmixing, and (g) proposed.

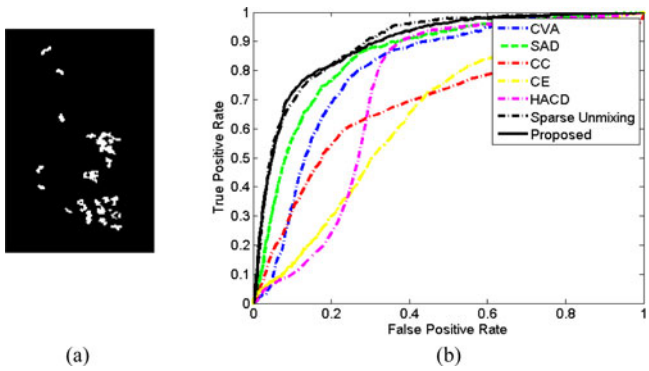

Fig. 21. Quantitative performance assessment for Blodgett dataset: (a) ground-truth map and (b) ROC curves.

pixels due to natural growth. The amount of changed pixels is very low compared to the total number of pixels, 2.82% of the pixels are subject to change.

Using the vegetation and volatiles signatures from the USGS spectral library, a spectral library of 224 spectra has been constructed for the sparse unmixing-based approaches. λ and λ_{TV} regularization parameters of SUnSAL-TV have been set as 0.001 and 0.01, after a crude empirical analysis.

The change maps obtained by CVA, SAD, CC, CE, HACD, sparse unmixing and sparse unmixing with dictionary pruning are provided in Fig. 20. A ground-truth change map has been prepared for this multitemporal dataset, based on difference operators on color space, thresholding, and binary morphology. It should be noted again that the authors do not claim that the presented ground-truth map is perfect or 100% correct. The

ground-truth map and the ROC curves obtained based on this map are provided in Fig. 21.

For this dataset, the proposed approach did not result in a performance enhancement with respect to sparse unmixing-based change detection without dictionary pruning step. However, dictionary pruning resulted in a computational time reduction from 710 to 206 s, of which the dictionary pruning step itself took around 2.1 s.

V. Conclusion and Future Research Lines

The numerous potentials and advantages of change detection by unmixing for multispectral hyperspectral data, with respect to traditional methods, have only recently begun to be investigated in detail. Sparse unmixing-based change detection is the most recent addition to the family of unmixing-based change detection approaches, and enables to use spectral libraries in the change detection process. With the increase in the number and availability of spectral libraries, sparse unmixing is bound to receive more and more attention in upcoming years. Sparse unmixing-based change detection, which involves both spectral and spatial processing, not only provides enhanced change detection performance (especially when the data contain subpixel-level changes), but also opens the door to applications that utilize dedicated spectral libraries, as is in the fields of environmental monitoring and defense. Nevertheless, sparse unmixing is overall an ill-conditioned and time-consuming problem due to large library sizes and high coherence. This paper proposed the utilization of a dictionary pruning approach with the recently proposed sparse unmixing-based change detection, to improve the conditioning of the unmixing process. The proposed approach not only decreases the computation time significantly, but also enhances the change detection performances even further, as evidenced by the presented synthetic and real data experiments. Possible future studies may aim to showcase the high performance of the proposed approach for dedicated applications and spectral libraries, or an investigation into the spectral library—data mismatch problem, which is a common point of concern for all sparse unmixing-based approaches.

Acknowledgment

The authors gratefully acknowledge the outstanding comments and suggestions provided by the Anonymous Reviewers, which greatly helped them to improve the technical quality and presentation of this paper.

References

[1] J. Meola, M. T. Eismann, R. L. Moses, and J. N. Ash, "Detecting changes in hyperspectral imagery using a model-based approach," *IEEE Trans. Geosci. Remote Sens.*, vol. 49, no. 7, pp. 2647–2661, Jul. 2011.

[2] A. Schaum and A. Stocker, "Long-interval chronochrome target detection," in *Proc. Int. Symp. Spectral Sens. Res.*, 1998.

[3] A. Schaum and A. Stocker, "Hyperspectral change detection and supervised matched filtering based on covariance equalization," *Proc. SPIE*, vol. 5425, pp. 77–90, 2004.

[4] J. Theiler and S. Perkins, "Proposed framework for anomalous change detection," in *Proc. ICML Workshop Mach. Learn. Algorithms Surveillance Event Detection*, Jun. 2006, pp. 7–14.

[5] C. Wu, B. Du, and L. Zhang, "A subspace-based change detection method for hyperspectral images," *IEEE J. Sel. Topics Appl. Earth Observ. Remote Sens.*, vol. 6, no. 2, pp. 815–830, Apr. 2013.

[6] A. A. Nielsen, K. Conradsen, and J. J. Simpson, "Multivariate alteration detection (MAD) and MAF post-processing in multispectral, bi-temporal image data: New approaches to change detection studies," *Remote Sens. Environ.*, vol. 64, pp. 1–19, 1998.

[7] A. A. Nielsen, "The regularized iteratively reweighted MAD method for change detection in multi- and hyperspectral data," *IEEE Trans. Image Process.*, vol. 16, no. 2, pp. 463–478, Feb. 2007.

[8] N. Keshava and J. F. Mustard, "Spectral unmixing," *IEEE Signal Process. Mag.*, vol. 19, no. 1, pp. 44–57, Jan. 2002.

[9] J. M. Bioucas-Dias *et al.*, "Hyperspectral unmixing overview: Geometrical, statistical, and sparse regression-based approaches," *IEEE J. Sel. Topics Appl. Earth Observ. Remote Sens.*, vol. 5, no. 2, pp. 354–379, Apr. 2012.

[10] Q. Du, L. Wassom, and R. King, "Unsupervised linear unmixing for change detection in multitemporal airborne hyperspectral imagery," in *Proc. Int. Workshop Anal. Multi-temporal Remote Sens. Images*, 2005, pp. 136–140.

[11] C.-C. Hsieh, P.-F. Hsieh, and C.-W. Lin, "Subpixel change detection based on abundance and slope features," in *Proc. IEEE Int. Geosci. Remote Sens. Symp.*, 2006, pp. 775–778.

[12] R. Zurita-Milla, L. Gomez-Chova, L. Guanter, J. G. P. W. Clevers, and G. Camps-Valls, "Multitemporal unmixing of medium-spatial-resolution satellite images: A case study using MERIS images for land-cover mapping," *IEEE Trans. Geosci. Remote Sens.*, vol. 49, no. 11, pp. 4308–4317, Nov. 2011.

[13] A. Ertürk and A. Plaza, "Informative change detection by unmixing for hyperspectral images," *IEEE Geosci. Remote Sens. Lett.*, vol. 12, no. 6, pp. 1252–1256, Jun. 2015.

[14] S. Liu, L. Bruzzone, F. Bovolo, and P. Du, "Unsupervised multitemporal spectral unmixing for detecting multiple changes in hyperspectral images," *IEEE Trans. Geosci. Remote Sens.*, vol. 54, no. 5, pp. 2733–2748, May 2016.

[15] A. Ertürk, M.-D. Iordache, and A. Plaza, "Sparse unmixing based change detection for multitemporal hyperspectral images," *IEEE J. Sel. Topics Appl. Earth Observ. Remote Sens.*, vol. 9, no. 2, pp. 708–719, Feb. 2016.

[16] M.-D. Iordache, J. M. Bioucas-Dias, and A. Plaza, "Sparse unmixing of hyperspectral data," *IEEE Trans. Geosci. Remote Sens.*, vol. 49, no. 6, pp. 2014–2039, Jun. 2011.

[17] K. Themelis, A. A. Rontogiannis, and K. Koutroumbas, "Semi-supervised hyperspectral unmixing through the weighted lasso," in *Proc. IEEE Int. Conf. Acoust., Speech, Signal Process.*, Dallas, TX, USA, Mar. 2010, pp. 1194–1197.

[18] J. M. Bioucas-Dias and M. Figueiredo, "Alternating direction algorithms for constrained sparse regression: Application to hyperspectral unmixing," in *Proc. 2nd Workshop Hyperspectral Image Signal Process.*, 2010, pp. 1–4.

[19] M.-D. Iordache, J. M. Bioucas-Dias, and A. Plaza, "Total variation spatial regularization for sparse hyperspectral unmixing," *IEEE Trans. Geosci. Remote Sens.*, vol. 50, no. 11, pp. 4484–4502, Nov. 2012.

[20] A. Chambolle, "An algorithm for total variation minimization and applications," *J. Math. Imag. Vis.*, vol. 20, nos. 1/2, pp. 89–97, Jan.–Mar. 2004.

[21] Y. Zhong, R. Feng, and L. Zhang, "Non-local sparse unmixing for hyperspectral remote sensing imagery," *IEEE J. Sel. Topics Appl. Earth Observ. Remote Sens.*, vol. 7, no. 6, pp. 1889–1909, Jun. 2014.

[22] M.-D. Iordache, J. M. Bioucas-Dias, and A. Plaza, "Dictionary pruning in sparse unmixing of hyperspectral data," in *Proc. 4th Workshop Hyperspectral Image Signal Process.: Evol. Remote Sens.*, 2012, pp. 1–4.

[23] J. M. Bioucas-Dias and J. M. P. Nascimento, "Hyperspectral subspace identification," *IEEE Trans. Geosci. Remote Sens.*, vol. 46, no. 8, pp. 2435–2445, Aug. 2008.

[24] *Hyperspectral Remote Sensing Scenes*, Comput. Intell. Group, Basque Univ., San Sebastián, Spain, 2015. [Online]. Available: http://www.ehu.es/ccwintco/index.php?title=Hyperspectral_Remote_Sensing_Scenes&redirect=no

[25] M. Bochow *et al.*, "Automatic shadow detection in hyperspectral VIS-NIR images," in *Proc. 7th EARSeL SIG Imag. Spectroscopy Workshop*, 2011.

[26] G. Tol, M. Shimoni, and J. Ahlberg, "A shadow detection method for remote sensing images using VHR hyperspectral and LIDAR data," in *Proc. IEEE Int. Geosci. Remote Sens. Symp.*, 2011, pp. 4423–4426.

[27] S. Adler-Golden, M. W. Matthew, G. P. Anderson, G. W. Felde, and J. A. Gardner, "Algorithm for de-shadowing spectral imagery," *Proc. SPIE*, vol. 4816, pp. 203–210, Nov. 2002.

[28] R. Richter and A. Müller, "De-shadowing of satellite/airborne imagery," *Int. J. Remote Sens.*, vol. 26, no. 15, pp. 3137–3148, 2005.

Alp Ertürk (S'11–M'14) received the B.Sc. and M.Sc. degrees in electrical and electronics engineering from Middle East Technical University, Ankara, Turkey, in 2007 and 2010, respectively, and the Ph.D. degree in electronics and telecommunication engineering from Kocaeli University, Kocaeli, Turkey, in 2013.

He was a Postdoctoral Researcher with the Hyperspectral Computing Laboratory (HyperComp), University of Extremadura, Cáceres, Spain. He is currently an Assistant Professor in the Department of Electronics and Telecommunication Engineering, Kocaeli University. His research interests are in the areas of digital image processing, remote sensing, and hyperspectral imaging.

Dr. Ertürk is a Reviewer for several journals including IEEE GEOSCIENCE AND REMOTE SENSING LETTERS, IEEE JOURNAL OF SELECTED TOPICS IN APPLIED EARTH OBSERVATIONS AND REMOTE SENSING, and *Journal of Applied Remote Sensing*. He is also currently serving as the Secretary and Treasurer of the IEEE GRSS Turkey Chapter.

Marian-Daniel Iordache received the M.Sc. degree in computer aided electrical engineering from the Faculty of Electrical Engineering, Politehnica University of Bucharest, Bucharest, Romania, in 2006, and the Ph.D. degree in electrical and computer engineering from the Instituto Superior Tecnico, Lisbon, Portugal, in 2011.

His research activity started in 2006 at the Electrical Engineering Research Center, Bucharest, where he worked on several national and European projects dedicated to microelectromechanical systems and high-frequency circuits. He is currently a Researcher in the Flemish Institute for Technological Research, Center for Remote Sensing and Earth Observation Processes (TAP), Mol, Belgium. His research is focused on hyperspectral data processing and unmixing, with emphasis on the sparse characteristics of the solutions.

Dr. Iordache was a Marie Curie Fellow with the Hyperspectral Imaging Network project funded by the European Commission under the Sixth Framework Programme from 2008 to 2011. Since 2010, he has been a member of the Hyperspectral Computing Laboratory Research Group, University of Extremadura, Cáceres, Spain. For his research activity and social implication, he was awarded with the prize The Romanian Student of the Year in Europe 2011, offered by the League of Romanian Students Abroad.

Antonio Plaza (M'05–SM'07–F'15) received the M.Sc. and Ph.D. degrees in computer engineering from the University of Extremadura, Badajoz, Spain, in 1999 and 2002, respectively.

He is currently working as the Head of the Hyperspectral Computing Laboratory, Department of Technology of Computers and Communications, University of Extremadura. He has authored more than 500 publications, including 182 JCR journal papers (132 in IEEE journals), 20 book chapters, and more than 250 peer-reviewed conference proceeding papers. He has guest edited nine special issues on hyperspectral remote sensing for different journals. He has reviewed more than 500 manuscripts for more than 50 different journals. His main research interests include hyperspectral data processing and parallel computing of remote sensing data.

Dr. Plaza is a Fellow of IEEE "for contributions to hyperspectral data processing and parallel computing of Earth observation data." He received the recognition of Best Reviewers of the IEEE GEOSCIENCE AND REMOTE SENSING LETTERS in 2009 and received the recognition of Best Reviewers of the IEEE TRANSACTIONS ON GEOSCIENCE AND REMOTE SENSING in 2010, for which he served as an Associate Editor in 2007.2012. He is also an Associate Editor for IEEE ACCESS and was a Member of the Editorial Board of the IEEE GEOSCIENCE AND REMOTE SENSING Newsletter (2011–2012) and the IEEE GEOSCIENCE AND REMOTE SENSING MAGAZINE in 2013. He was also a Member of the steering committee of the IEEE JOURNAL OF SELECTED TOPICS IN APPLIED EARTH OBSERVATIONS AND REMOTE SENSING (JSTARS). He received the Best Column Award of the IEEE SIGNAL PROCESSING MAGAZINE in 2015, the 2013 Best Paper Award of the JSTARS journal, and the most highly cited paper in the JOURNAL OF PARALLEL AND DISTRIBUTED COMPUTING from 2005 to 2010. He received the best paper awards at the IEEE International Conference on Space Technology and the IEEE Symposium on Signal Processing and Information Technology. In 2011.2012, he was the Director of Education Activities for the IEEE Geoscience and Remote Sensing Society (GRSS) and is currently serving as the President of the Spanish Chapter of IEEE GRSS. He is currently serving as the Editor-in-Chief of the IEEE TRANSACTIONS ON GEOSCIENCE AND REMOTE SENSING JOURNAL.